

A $\{\text{Fe}(\text{NO})_3\}^{10}$ Trinitrosyliron Complex Stabilized by an N-Heterocyclic Carbene and the Cationic and Neutral $\{\text{Fe}(\text{NO})_2\}^{9/10}$ Products of Its NO Release

Chung-Hung Hsieh and Marcetta Y. Darensbourg*

Department of Chemistry, Texas A&M University, College Station, Texas 77843

Received May 13, 2010; E-mail: marcetta@mail.chem.tamu.edu

Abstract: In contrast to the instability of $\text{XFe}(\text{NO})_3$ and $[\text{R}_3\text{PFe}(\text{NO})_3]^+$, the N-heterocyclic carbene (NHC)-containing trinitrosyliron complex (TNIC) $[(\text{IMes})\text{Fe}(\text{NO})_3][\text{BF}_4]$ (**1**) [$\text{IMes} = 1,3\text{-bis}(2,4,6\text{-trimethylphenyl})\text{imidazol-2-ylidene}$] can be readily isolated and manipulated in solution under ambient conditions. Nevertheless, in the presence of thiolates (SR^-), this EPR-silent TNIC (denoted $\{\text{Fe}(\text{NO})_3\}^{10}$ in the Enemark–Feltham notation) releases gaseous NO, affording in the case of $\text{SR}^- = \text{SPh}^-$ the EPR-active, neutral dinitrosyliron complex (DNIC) $(\text{IMes})\text{Fe}(\text{SPh})(\text{NO})_2$ (**3**, $\{\text{Fe}(\text{NO})_2\}^9$). Carbon monoxide enforces a bimolecular reductive elimination of PhSSPh from **3**, yielding $(\text{IMes})(\text{CO})\text{Fe}(\text{NO})_2$ (**2**), a reduced $\{\text{Fe}(\text{NO})_2\}^{10}$ DNIC. The NO released from TNIC **1** in the presence of SPh^- could be taken up by the NO-trapping agent $[(\text{bme-dach})\text{Fe}]_2$ [$\text{bme-dach} = N,N\text{-bis}(2\text{-mercaptoethyl})\text{-}1,4\text{-diazacycloheptane}$] to form the mononitrosyliron complex (MNIC) $(\text{bme-dach})\text{Fe}(\text{NO})$. In the absence of SPh^- , direct mixing of $[(\text{bme-dach})\text{Fe}]_2$ with **1** releases both NO and the NHC with formation of a spin-coupled, diamagnetic $\{\text{Fe}(\text{NO})\}^7\text{-}\{\text{Fe}(\text{NO})_2\}^9$ complex, $[(\text{NO})\text{Fe}(\text{bme-dach})\text{Fe}(\text{NO})_2][\text{BF}_4]$ (**4**). In **4**, the MNIC serves as a bidentate metallothiolate ligand of $\text{Fe}(\text{NO})_2$, forming a butterfly complex in which the Fe–Fe distance is 2.7857(8) Å. Thus, **1** is found to be a reliable synthon for $[\{\text{Fe}(\text{NO})_2\}^9]^+$. The solid-state molecular structures of complexes **1–3** show that all three complexes have a tetrahedral geometry in which the bulky mesitylene substituents of the carbene ligand appear to umbrella the $\text{Fe}(\text{NO})_2\text{L}$ [$\text{L} = \text{NO}$ (**1**), CO (**2**), SPh (**3**)] motif.

Introduction

Positioned as it is between its one-electron redox partners NO^+ and NO^- , the electronic state of the NO radical as a ligand is highly influenced by the transition metal to which it binds and by ancillary ligands.¹ While the oxidation-state assignment of the metal in such complexes is arguable, a general rule for organometallic-like complexes is that two nitrosyls ($\text{NO}\cdot$ is a three-electron donor) correspond with three carbonyls in the electron count. Thus, from $\text{Fe}(\text{CO})_5$, the diamagnetic 18-electron dinitrosyliron complex (DNIC) $\text{Fe}(\text{CO})_2(\text{NO})_2$ is derived; $\text{Cr}(\text{NO})_4$ is the homoleptic analogue of $\text{Cr}(\text{CO})_6$. Tetrahedral $\text{Mn}(\text{CO})(\text{NO})_3$ and $\text{XFe}(\text{NO})_3$ ($\text{X} = \text{I}^-, \text{Br}^-, \text{Cl}^-, \text{FBF}_3^-, \text{EtCN}$) exemplify 16-electron $[\text{M}(\text{NO})_3]^n$ fragments with $n = 0$ and $1+$, respectively.^{2–4}

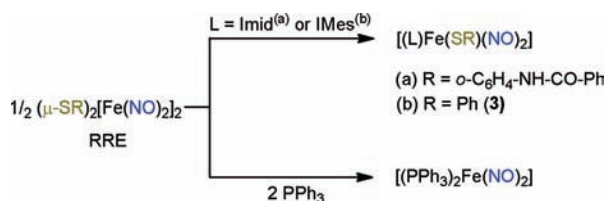
Of great current interest are DNICs found in biology as paramagnetic $[(\text{CysS})_2\text{Fe}(\text{NO})_2]^-$,⁵ either protein-bound or in

mobile low-molecular-weight forms.⁶ Electronic descriptions of the anionic dithiolates vary from $\text{Fe}^{\text{I}}(\text{NO})_2^7$ to a 17-electron species containing the 13-electron $\text{Fe}(\text{NO})_2^+$ unit; in the Enemark–Feltham (E.–F.) electronic notation, the latter is oxidized $\{\text{Fe}(\text{NO})_2\}^9$.^{8,9} Such DNICs are expected to be physiologically significant as products of iron–sulfur cluster degradation^{10,11} or as NO-storage and -transport agents. Synthetic analogues have been suggested as possible NO-release pharmaceutical agents.^{12–14} Mononitrosyliron complexes (MNICs)

- (1) Richter-Addo, G. B.; Legzdins, P.; Burstyn, J. *Chem. Rev.* **2002**, *102*, 857–860.
- (2) Hedberg, L.; Hedberg, K.; Satija, S. K.; Swanson, B. I. *Inorg. Chem.* **1985**, *24*, 2766–2771.
- (3) Hayton, T. W.; McNeil, W. S.; Patrick, B. O.; Legzdins, P. *J. Am. Chem. Soc.* **2003**, *125*, 12935–12944.
- (4) Beck, W.; Klapötke, T. M.; Mayer, P. Z. *Anorg. Allg. Chem.* **2006**, *632*, 417–420.
- (5) (a) Vithayathil, A. J.; Ternberg, J. L.; Commoner, B. *Nature* **1965**, *207*, 1246–1249. (b) Woolum, J. C.; Commoner, B. *Biochim. Biophys. Acta* **1970**, *201*, 131–140.

- (6) Cesareo, E.; Parker, L. J.; Pedersen, J. Z.; Nuccetelli, M.; Mazzetti, A. P.; Pastore, A.; Federici, G.; Caccuri, A. M.; Ricci, G.; Adams, J. J.; Parker, M. W.; Bello, M. L. *J. Biol. Chem.* **2005**, *280*, 42172–42180.
- (7) Vanin, A. F.; Poltorakov, A. P.; Mikoyan, V. D.; Kubrina, L. N.; Burbaev, D. S. *Nitric Oxide* **2010**, *23*, 136–149.
- (8) Enemark, J. H.; Feltham, R. D. *Coord. Chem. Rev.* **1974**, *13*, 339–406.
- (9) Ye, S.; Neese, F. *J. Am. Chem. Soc.* **2010**, *132*, 3646–3647.
- (10) (a) Ding, H.; Demple, B. *Proc. Natl. Acad. Sci. U.S.A.* **2000**, *97*, 5146–5150. (b) Yang, W.; Rogers, P. A.; Ding, H. *J. Biol. Chem.* **2002**, *277*, 12868–12873.
- (11) Foster, M. W.; Cowan, J. A. *J. Am. Chem. Soc.* **1999**, *121*, 4093–4100.
- (12) Vanin, A. F.; Mikoyan, V. D.; Kubrina, L. H. *Mol. Biophys.* **2010**, *55*, 5–12.
- (13) (a) Chen, Y.-J.; Ku, W.-C.; Feng, L.-T.; Tsai, M.-L.; Hsieh, C.-H.; Hsu, W.-H.; Liaw, W.-F.; Hung, C.-H.; Chen, Y.-J. *J. Am. Chem. Soc.* **2008**, *130*, 10929–10938. (b) Chang, H.-H.; Hung, H.-J.; Ho, Y.-L.; Wen, Y.-D.; Huang, W.-N.; Chiou, S.-J. *Dalton Trans.* **2009**, 6396–6402. (c) Lu, T.-T.; Chiou, S.-J.; Chen, C.-Y.; Liaw, W.-F. *Inorg. Chem.* **2006**, *45*, 8799–8806.
- (14) Dillinger, S. A. T.; Schmalle, H. W.; Fox, T.; Berke, H. *Dalton Trans.* **2007**, 3562–3571.

Scheme 2



graphically characterized neutral (L)(X)Fe(NO)₂ compounds, the imidazole (Imid) derivative (Imid)(S-Aryl)Fe(NO)₂ (S-Aryl = 2-benzamidobenzenethiolate) appears to be the closest analogue of **3**.^{22d} Notably, both (Imid)(S-Aryl)Fe(NO)₂ and **3** can be obtained by cleavage of the appropriate Roussin's red "esters" (RREs), (μ-S-Aryl)₂[Fe(NO)₂]₂ and (μ-S-Ph)₂[Fe(NO)₂]₂, by imidazole and the IMes carbene ligand, respectively (Scheme 2). These reactions contrast with RRE cleavage by phosphines, in which concomitant reductive elimination of RSSR leads to the reduced {Fe(NO)}¹⁰-containing DNIC (R₃P)₂Fe(NO)₂, as also shown in Scheme 2.²³

Electrochemistry of Complexes 1–3. Cyclic voltammograms of complexes **1**, **2**, and **3** were recorded in 2 mM THF solutions with 100 mM [*n*-Bu₄N][BF₄] as the supporting electrolyte; the potentials were measured relative to a Ag/AgNO₃ electrode using a glassy carbon electrode and are referenced to Cp₂Fe/Cp₂Fe⁺ (*E*_{1/2} = 0.00 V vs Ag/AgNO₃ in THF). For complex **1**, reversible or quasi-reversible redox processes are centered at −0.29 and −1.13 V, respectively (Figure 2a). The latter feature broadened in repeated scans, and its reversibility was not improved upon scan reversal at −1.9 V (Figure S11 in the Supporting Information). The reversible event is assigned to the {Fe(NO)₃}^{10/11} couple. While the more negative event is most likely a result of decomposition, it is not the NO⁺/NO couple.

The only redox feature of complex **2** within the solvent window is an irreversible oxidation at −0.34 V (Figure 2b). For complex **3**, a process centered at −1.48 V was scan-rate-independent (Figure 2c) and is assigned to the {Fe(NO)₂}^{9/10} couple. Its *i*_{pa}/*i*_{pc} ratio of 0.98 (at a scan rate of 100 mV/s) indicates reversibility, even though the separation of the *E*_{pa} and *E*_{pc} maxima is ~380 mV. As the Fc/Fc⁺ standard shows a similar separation under these conditions (Figure S10 in the Supporting Information), good reversibility is indicated. The greater accessibility of the reductive couple of the TNIC relative to the DNIC is consistent with the cationic charge of the former.

Electron Paramagnetic Resonance Spectroscopy Studies. The EPR spectrum of complex **3** shows an isotropic signal at *g* = 2.032 that is typical of {Fe(NO)₂}⁹ DNICs at RT (Figure 3). Rhombicity is seen for **3** at 77 K with the following *g* values: *g*₁ = 2.049, *g*₂ = 2.029, *g*₃ = 2.013 (Figure 3).^{5,22} Complexes **1** and **2** are diamagnetic, indicating reduced states of {Fe(NO)₂}¹⁰ and {Fe(NO)₃}¹⁰, respectively. That is, CO replacement by NO⁺ in the synthesis of TNIC **1** produced the same overall E.–F. electron count as in the reduced dinitrosyliron unit.⁸

Molecular Structures. X-ray-quality green crystals of TNIC **1** were isolated from THF/pentane, and the molecular structure of **1** obtained from them is presented in Figure 4a. DNICs **2** and **3** were obtained as brown and purple crystals, respectively, and their molecular structures are compared in Figure 4b,c. All may be considered as tetrahedral complexes, with the CN₂C₂ plane of the NHC bisecting the L–Fe–L angles of the trigonal base. The planes of the mesitylenes are roughly perpendicular to the CN₂C₂ plane and appear to umbrella the Fe(NO)₂L fragment. The Fe–N–O angles in **1** and **2** (avg. 174.3°) are more linear than those in **3**; the average angles of 168.7° in **3** orient the two N–O ligands inward toward each other in the

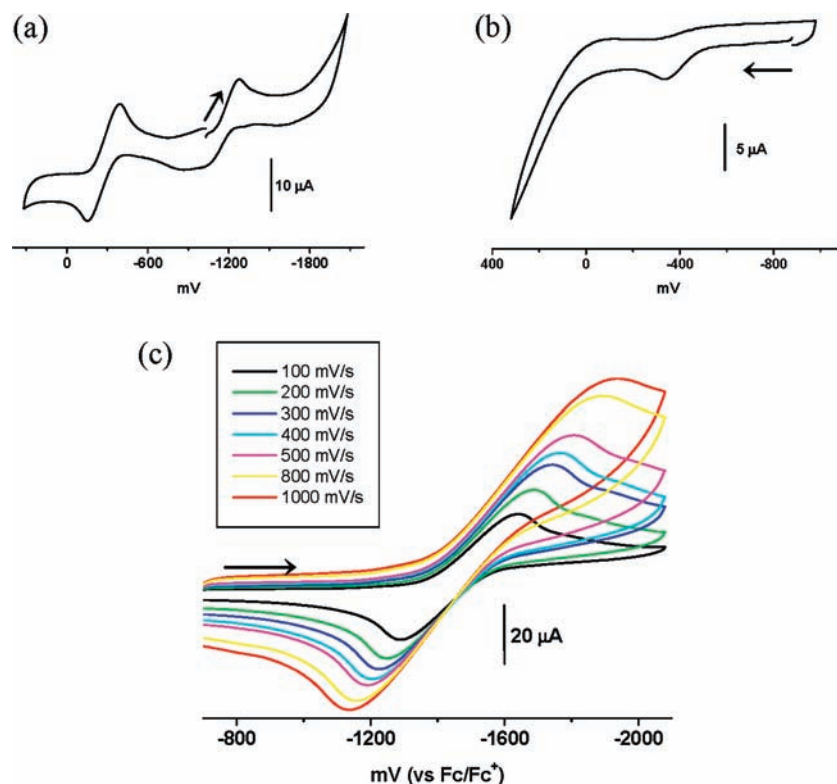


Figure 2. Cyclic voltammograms of (a) **1** and (b) **2** at scan rates of 200 and 100 mV/s, respectively, and (c) **3** at scan rates of 100–1000 mV/s in 2 mM THF solution.

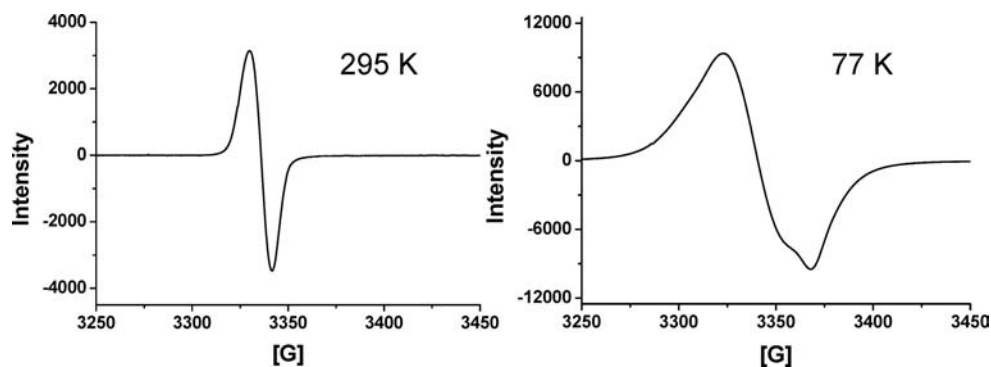


Figure 3. X-band EPR spectra of complex **3** in THF solution at 295 K ($g = 2.032$) and 77 K ($g_1 = 2.049$, $g_2 = 2.029$, $g_3 = 2.013$).

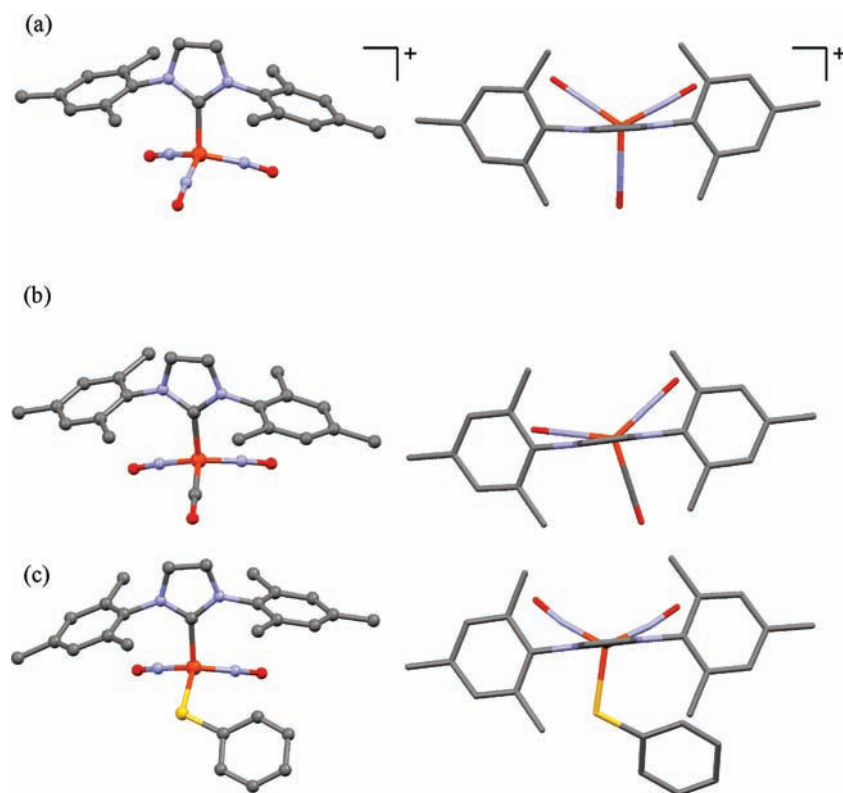


Figure 4. Molecular structures of (a) **1** (the BF_4^- counterion and H_2O packing solvent have been omitted), (b) **2**, and (c) **3** (the H_2O solvent of crystallization has been omitted): (left) side views as ball-and-stick renditions; (right) top views as capped-stick renditions. Thermal ellipsoid plots are provided in the Supporting Information.

“attracto” configuration.²³ Table 1 lists selected bond distances and angles in complexes **1–3**. It should be noted that the trend of decreasing Fe–N bond distances across the series **1**, **2**, and **3** is consistently accompanied by an increase in N–O distance, as expected on the basis of back-bonding arguments.

Comparison of 1 to the Phosphine Derivative $[(p\text{-tolyl})_3\text{P}]\text{Fe}(\text{NO})_3[\text{BF}_4]$. In order to understand the stability and chemical properties of TNIC **1**, $[(p\text{-tolyl})_3\text{P}]\text{Fe}(\text{NO})_3[\text{BF}_4]$ was prepared by procedures similar to those described for **1** (Scheme 3). Upon addition of $(p\text{-tolyl})_3\text{P}$ to a THF solution of $\text{Fe}(\text{CO})_2(\text{NO})_2$ in 1:1 stoichiometry, a reaction ensued over the course of 10 min that yielded the thermally stable, neutral complex $(p\text{-tolyl})_3\text{P}(\text{Fe}(\text{CO})(\text{NO})_2)_2$, a $\{\text{Fe}(\text{NO})_2\}^{10}$ species with $\nu(\text{NO})$ and $\nu(\text{CO})$ absorptions analogous to those of $(\text{Ph}_3\text{P})\text{Fe}(\text{CO})(\text{NO})_2$.^{23b,24}

Mixing of $(p\text{-tolyl})_3\text{P}(\text{Fe}(\text{CO})(\text{NO})_2)$ with 1 equiv of $[\text{NO}]\text{BF}_4$ in diethyl ether resulted in the precipitation of $[(p\text{-tolyl})_3\text{P}]\text{Fe}(\text{NO})_3[\text{BF}_4]$ as the reaction occurred. The product was isolated as a diamagnetic green solid and characterized by elemental analysis and IR spectroscopy.¹⁴

The solid-state attenuated total reflection IR (ATR-IR) spectra in the $\nu(\text{NO})$ region of $[(p\text{-tolyl})_3\text{P}]\text{Fe}(\text{NO})_3^+$ and complex **3**

(21) Chiang, C.-Y.; Miller, M. L.; Reibenspies, J. H.; Darensbourg, M. Y. *J. Am. Chem. Soc.* **2004**, *126*, 10867–10874.

(22) (a) Tsai, M.-C.; Tsai, F.-T.; Lu, T.-T.; Tsai, M.-L.; Wei, Y.-C.; Hsu, I.-J.; Lee, J.-F.; Liaw, W.-F. *Inorg. Chem.* **2009**, *48*, 9579–9591. (b) Tsai, F.-T.; Kuo, T.-S.; Liaw, W.-F. *J. Am. Chem. Soc.* **2009**, *131*, 3426–3427. (c) Tsai, M.-L.; Hsieh, C.-H.; Liaw, W.-F. *Inorg. Chem.* **2007**, *46*, 5110–5117. (d) Tsai, M.-L.; Liaw, W.-F. *Inorg. Chem.* **2006**, *45*, 6583–6585.

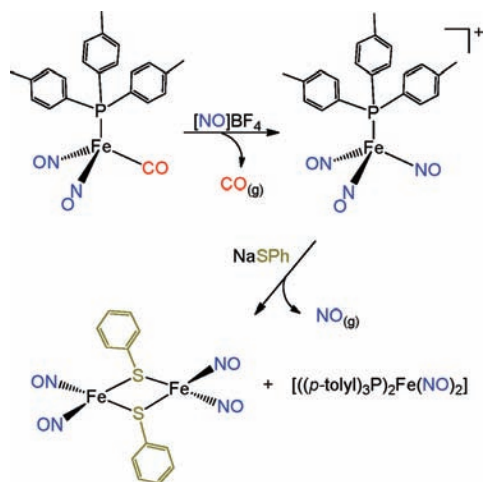
(23) (a) Reginato, N.; McCrory, C. T. C.; Pervitsky, D.; Li, L. *J. Am. Chem. Soc.* **1999**, *121*, 10217–10218. (b) Li, L.; Reginato, N.; Urschey, M.; Stradiotto, M.; Liarakos, J. D. *Can. J. Chem.* **2003**, *81*, 478–475.

(24) Atkinson, F. I.; Blackwell, H. E.; Brown, N. C.; Connelly, N. G.; Crossley, J. G.; Orpen, A. G.; Rieger, A. L.; Rieger, P. H. *J. Chem. Soc., Dalton Trans.* **1996**, 3491–3502.

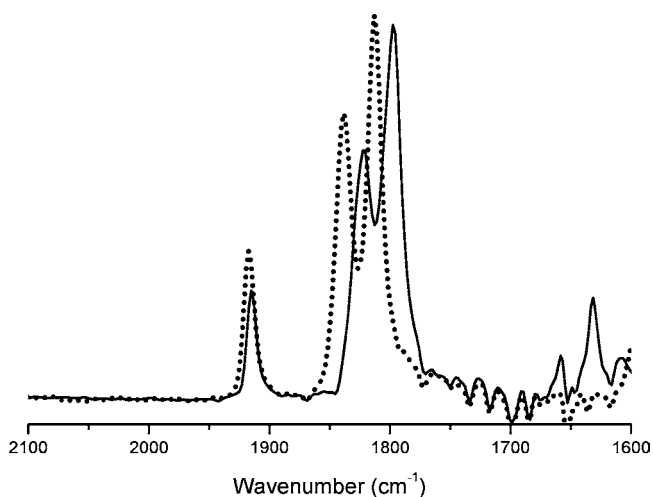
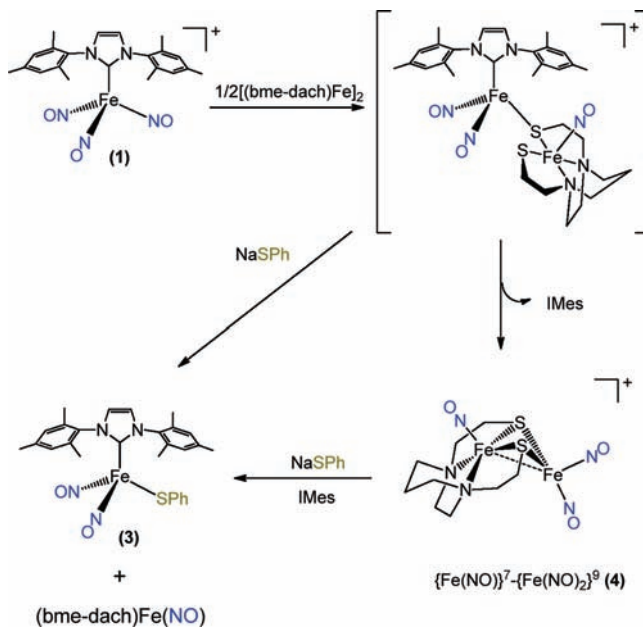
Table 1. Selected Bond Distances and Angles in Complexes **1**, **2**, and **3**

	1	2	3
Bond Distances (Å)			
Fe–C _{carb}	1.999(5)	1.989(3)	2.045(3)
Fe–NO ^a	1.689(5)	1.676(3)	1.672(3)
Fe–CO	–	1.777(4)	–
Fe–S	–	–	2.2532(17)
N–O	1.147(6)	1.184(3)	1.182(3)
	1.140(6)	1.164(3)	1.186(3)
	1.144(6)		
Bond Angles (deg)			
N–Fe–N	112.7(2) ^a	119.78(12)	115.76(13)
Fe–N–O ^a	173.5(5)	175.2(2)	168.7(2)
C _{carb} –Fe–NO ^a	106.02(5)	107.72(10)	107.28(11)
C _{carb} –Fe–S	–	–	109.13(9)
C _{carb} –Fe–CO	–	101.52(12)	–

^a Average values. The maximum deviations from the average distances and angles are shown in the table. Full lists of metric parameters are given in the Supporting Information

Scheme 3

are compared in Figure 5. The two bands (A and E) expected for ideal C_{3v} symmetry show a splitting of the E mode for both TNICs, as was also reported for $[(HOCH_2)_3P]Fe(NO)_3]^+$.¹⁴ As displayed in Figure 5, the solid-state $\nu(NO)$ bands of $[(p\text{-tolyl})_3P]Fe(NO)_3]^+$ at 1917 (s), 1838 (vs), and 1813 (vs) cm^{-1}

**Figure 5.** Overlaid $\nu(NO)$ solid-state ATR-IR spectra of **1** (solid line) and $[(p\text{-tolyl})_3P]Fe(NO)_3]^+$ (dotted line).**Scheme 4**

have higher frequencies than the corresponding bands of **1** [1916 (s), 1823 (vs), and 1799 (vs) cm^{-1}], indicating the greater donating ability of the NHC ligand. A similar conclusion is derived from the CO-containing DNIC analogues in THF solution: $\nu(CO) = 2005$ (s) cm^{-1} and $\nu(NO) = 1762$ (s), 1720 (vs) cm^{-1} for $((p\text{-tolyl})_3P)Fe(CO)(NO)_2$ versus $\nu(CO) = 1986$ (s) and $\nu(NO) = 1744$ (s), 1702 (vs) cm^{-1} for **2**.

Nitric Oxide Release and Capture by a NO-Trapping Agent.

The NO-release activity of **1** was assessed by the procedure of Tsai, Chen, and Liaw.²⁵ In an Ar-filled glovebox, a small open vial containing solids **1** and NaSPh was placed in a larger tube containing a known NO-trapping agent, $[(bme\text{-dach})Fe]_2$ [bme-dach = *N,N'*-bis(2-mercaptoethyl)-1,4-diazacycloheptane], dissolved in MeOH (Scheme 1).²⁶ Upon injection of THF through the septum-sealed tube into the small vial, the outer brown solution changed to green over a few hours. The IR spectrum of the contents of the outer tube indicated the formation of $(bme\text{-dach})Fe(NO)$ [$\nu(NO) = 1647$ cm^{-1}],²⁶ while complex **3** was observed to form in the vial.

Direct mixing of $[(bme\text{-dach})Fe]_2$ and complex **1** rapidly resulted in NO release/transfer (Scheme 4). In the absence of SPh^- , an NO-containing product, complex **4**, was detected as an EPR-silent species with $\nu(NO)$ values of 1795 (s), 1763 (s), and 1740 (vs) cm^{-1} (THF solution). Addition of SPh^- to the reaction mixture converted the species to DNIC **3** with release of the MNIC $(bme\text{-dach})Fe(NO)$. Positive-ion-mode electrospray ionization mass spectrometry (ESI-MS⁺) of the product, which was isolated as a dark-brown solid in the absence of SPh^- , showed a parent peak at m/z 419.9, with fragments at m/z 389.9 and 359.9 representing the successive losses of one and two NO groups, respectively. The composition of the final product and its structure were confirmed by X-ray crystallography. As also shown in Scheme 4, a mixture of NaSPh and the IMes ligand converted isolated **4** to complex **3** and the MNIC.

The structure of complex **4** is that of a butterfly complex in which the bridging thiolate sulfurs form the hinge (Figure 6).

(25) Tsai, F.-T.; Chen, P.-L.; Liaw, W.-F. *J. Am. Chem. Soc.* **2010**, *132*, 5290–5299.

(26) Chiang, C.-Y.; Lee, J.; Dalrymple, C.; Sarahan, M. C.; Reibenspies, J. H.; Darensbourg, M. Y. *Inorg. Chem.* **2005**, *44*, 9007–9016.

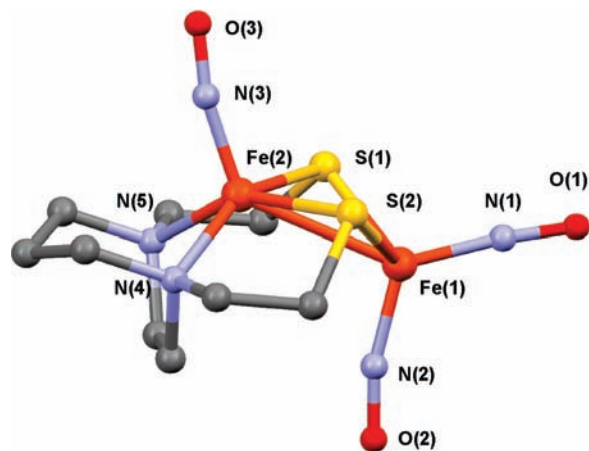


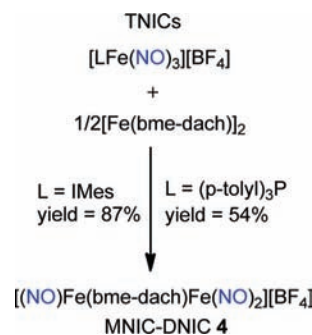
Figure 6. Molecular structure of complex **4** (the BF_4^- counterion has been omitted) as a ball-and-stick view. Thermal ellipsoid plots and a full list of metric parameters are provided in the Supporting Information. Selected bond distances (Å) and angles (deg): Fe(1)–Fe(2), 2.7857(8); Fe(1)–N(1), 1.669(2); Fe(1)–N(2), 1.673(2); Fe(1)–S(1), 2.2516(9); Fe(1)–S(2), 2.2469(9); Fe(2)–N(3), 1.668(2); Fe(2)–S(1), 2.2435(8); Fe(2)–S(2), 2.2590(8); Fe(2)–N(4), 2.0369(19); Fe(2)–N(5), 2.026(2); N(1)–O(1), 1.174(3); N(2)–O(2), 1.169(3); N(3)–O(3), 1.147(3); $\angle\text{Fe(1)–N(1)–O(1)}$, 174.40(19); $\angle\text{Fe(1)–N(2)–O(2)}$, 166.6(2); $\angle\text{Fe(2)–N(3)–O(3)}$, 165.8(2); $\angle\text{N(1)–Fe(1)–N(2)}$, 116.63(10); $\angle\text{Fe(1)–S(1)–Fe(2)}$, 76.59(3); $\angle\text{Fe(1)–S(2)–Fe(2)}$, 76.37(3); $\angle\text{S(1)–Fe(1)–S(2)}$, 92.63(3); $\angle\text{S(1)–Fe(2)–S(2)}$, 92.52(3); $\angle\text{N(4)–Fe(2)–N(5)}$, 78.50(8).

Selected metric parameters are given in the figure caption, the most notable being the Fe–Fe distance of 2.7857(8) Å. The Fe–N–O angle of the MNIC portion of the diiron complex is 165.8(2)°, while the Fe–N–O angles in the DNIC average to 170.5(2)°. The N_2S_2 donor set forms a precise square plane with deviations of no more than ± 0.005 Å. The Fe is displaced from this plane by 0.524 Å, with the NO positioned on the 3-carbon side of the dach diazacycle. While it is related to the structure of the dithiolato-S-bridged $\{\text{Fe}(\text{NO})\}^7-\{\text{Fe}(\text{NO})_2\}^9$ compound characterized by Liaw's group [$\text{Fe}\cdots\text{Fe}$ distance = 2.6688(5) Å],²⁷ the structure of **4** is also similar to the dithiolato-bridged $(\text{NiN}_2\text{S}_2)\{\text{Fe}(\text{NO})_2\}^{10}$ complex reported by Osterloh et al.,²⁸ in which the Ni–Fe distance is 2.797(1) Å. In that case, the $\nu(\text{NO})$ values of the $\text{Fe}(\text{NO})_2$ unit are 1663 and 1624 cm^{-1} , i.e., some 100 cm^{-1} lower than those of the cationic complex **4**. From the $\nu(\text{NO})$ intensity pattern of complex **4**, as well as the band separation, we assign the IR bands at 1795 and 1740 cm^{-1} to the $\text{Fe}(\text{NO})_2$ unit, while the central band at 1763 cm^{-1} would be the $\nu(\text{NO})$ of the MNIC portion of complex **4**.

That the (bme-dach)Fe(NO) complex can act as a metallodithiolate ligand has been established in the case of a $\text{W}(\text{CO})_4$ adduct, whose paramagnetism derives from the $\{\text{Fe}(\text{NO})\}^7$ unit.²⁹ In that example, the $\nu(\text{NO})$ of the MNIC is 1697 cm^{-1} , which is positively shifted by 50 cm^{-1} from the value for the free (bme-dach)Fe(NO) complex (1647 cm^{-1}).²⁹ As the electron-withdrawing ability of the cationic $\{\text{Fe}(\text{NO})_2\}^9$ unit is stronger than that of neutral $\text{W}(\text{CO})_4$, the much larger shift observed for $\nu(\text{NO})$ of the MNIC in complex **4** (the 1763 cm^{-1} absorption) is as expected.^{26,29}

- (27) Chen, H.-W.; Lin, C.-W.; Chen, C.-C.; Yang, L.-B.; Chiang, M.-H.; Liaw, W.-F. *Inorg. Chem.* **2005**, *44*, 3226–3232.
 (28) Osterloh, F.; Saak, W.; Haas, D.; Pohl, S. *Chem. Commun.* **1997**, 979–980.
 (29) Hess, J. L.; Conder, H. L.; Green, K. N.; Darensbourg, M. Y. *Inorg. Chem.* **2008**, *47*, 2056–2063.

Scheme 5



Conclusions

Despite the popularity and rapid rise of N-heterocyclic carbene ligands to preeminence in catalysis,^{30,31} to our knowledge this is the first description of their use in nitrosyliron biomimetic complexes. The clarity of the transformations described above, which interconvert the TNIC with DNICs at two redox levels, $\{\text{Fe}(\text{NO})_2\}^9$ and $\{\text{Fe}(\text{NO})_2\}^{10}$, capitalizes on the ability of the NHC to bind to both harder and softer metal sites and differs significantly from the behavior of known phosphine TNICs. In contrast to the solution stability of **1**, $[(p\text{-tolyl})_3\text{P}]\text{Fe}(\text{NO})_3]^+$ decomposes immediately upon attempts to dissolve it in THF (at either 22 or 0 °C). In the presence of NaSPh, the decomposition products of phosphine TNICs are mixtures of $(\mu\text{-SPh})_2[\text{Fe}(\text{NO})_2]_2$ and $((p\text{-tolyl})_3\text{P})_2\text{Fe}(\text{NO})_2$ (Scheme 2). That is, the phosphine is not a tenacious binder of $[\text{Fe}(\text{NO})_2]^+$, as is the NHC. In the case of direct mixing of the NO trapping agent $[(\text{bme-dach})\text{Fe}]_2$ with either $[(p\text{-tolyl})_3\text{P}]\text{Fe}(\text{NO})_3][\text{BF}_4]$ or TNIC **1**, the same diiron complex **4** is obtained. However, the yield in the former case is some 30% less because of the rapid decomposition of the TNIC source of NO and $[\text{Fe}(\text{NO})_2]^+$ (Scheme 5). We thus conclude that the TNIC **1** provides a robust synthon for the paramagnetic $[\{\text{Fe}(\text{NO})_2\}^9]^+$ unit and offers potential as a spin-probe source in biological studies. It also presents a significant opportunity for mechanistic explorations of both NO delivery and redox-level interconversions in the $\text{Fe}(\text{NO})_2$ unit.

The enormous effort that has been directed toward functionalization of NHCs, including control of lipophilicity and hydrophilicity,^{32,33} and the possibility of NHC attachment to supports, biomolecules, and nanoparticles, suggest that further development of such fundamental chemistry as described above can be within the design strategy for targeted pharmaceuticals or sensors based on NO or $\text{Fe}(\text{NO})_2$.^{33,34}

Experimental Section

General Materials and Techniques. All reactions and operations were carried out on a double-manifold Schlenk vacuum line under a N_2 or Ar atmosphere. THF, CH_2Cl_2 , pentane, and diethyl ether were freshly purified by an MBraun manual solvent purification system packed with Alcoa F200 activated alumina desiccant. The purified THF, CH_2Cl_2 , pentane, and diethyl ether were stored

- (30) Gusev, D. G. *Organometallics* **2009**, *28*, 6458–6461.
 (31) Cornils, B.; Herrmann, W. A. *Aqueous-Phase Organometallic Catalysis*, 2nd ed.; Wiley-VCH: Weinheim, Germany, 2004.
 (32) Hong, S. H.; Grubbs, R. H. *J. Am. Chem. Soc.* **2006**, *128*, 3508–3509.
 (33) Hindi, K. M.; Panzner, M. J.; Tessier, C. A.; Cannon, C. L.; Youngs, W. J. *Chem. Rev.* **2009**, *109*, 3859–3884.
 (34) (a) Tonzetich, Z. J.; McQuade, L. E.; Lippard, S. J. *Inorg. Chem.* **2010**, *49*, 6338–6348. (b) McQuade, L. E.; Lippard, S. J. *Inorg. Chem.* **2010**, *49*, 7464–7471.

with molecular sieves under N₂ before experiments. The known complex Fe(CO)₂(NO)₂ and the NO trapping agent [(bme-dach)Fe]₂ were synthesized using published procedures.^{25,35} The following materials were reagent-grade and used as purchased from Sigma-Aldrich: sodium thiophenolate, sodium *tert*-butoxide, 1,3-bis(2,4,6-trimethylphenyl)imidazolium chloride, nitrosyl tetrafluoroborate, and tri-*p*-tolylphosphine.

Physical Measurements. ¹H NMR spectra were measured on a Unity+ 300 MHz superconducting NMR instrument. Solution IR spectra were recorded on a Bruker Tensor 27 FTIR spectrometer using 0.1 mm KBr sealed cells. All of the electrochemical analyses were done using a Bioanalytical Systems 100 electrochemical workstation with a glassy carbon working electrode and a platinum wire auxiliary electrode. All voltammograms were obtained using a standard three-electrode cell under an Ar atmosphere at room temperature. All samples in THF were run at a concentration of 2 mM with [*n*-Bu₄N][BF₄] as the supporting electrolyte (100 mM), and potentials are reported relative to the Fc/Fc⁺ couple as 0.00 V. The rest potential for complex **1** was found to be +0.056 V. Elemental analyses were performed by Atlantic Microlab, Inc. (Norcross, GA).

X-band EPR measurements were performed using a Bruker EMX spectrometer equipped with an ER4102ST cavity and an Oxford Instruments ESR900 cryostat. The microwave frequency was measured with a Hewlett-Packard 5352B electronic counter. X-band spectra of complex **3** in THF solution were collected with microwave powers of 0.2012 and 0.02012 mW and frequencies of 9.487 and 9.4730 GHz at 295 and 77 K, respectively, and a modulation amplitude of 10 G at 100 kHz.

ESI-MS analysis was performed using an API QStar Pulsar, MDS Sciex (Toronto, ON) quadrupole–TOF hybrid mass spectrometer. Gas chromatography–mass spectrometry was performed on an Ultra Trace GC attached to a DSQII quadrupole mass spectrometer (Thermo Electron Corporation (Austin, TX)). The mass spectrometer was operated in electron impact ionization mode at 70 eV electron energy.

X-ray Crystal Structure Analyses. A Bausch and Lomb 10× microscope was used to identify suitable crystals of the same habit. Each crystal was coated in paratone, affixed to a Nylon loop, and placed under streaming nitrogen (110 K) in a Bruker SMART 1000 CCD or SMART Apex CCD diffractometer (for details, see the CIFs in the Supporting Information). The space groups were determined on the basis of systematic absences and intensity statistics. The structures were solved by direct methods and refined by full-matrix least-squares on *F*². Anisotropic displacement parameters were determined for all non-hydrogen atoms. Hydrogen atoms were placed at idealized positions and refined with fixed isotropic displacement parameters. The following is a list of programs used: data collection and cell refinement, SMART WNT/2000, version 5.632,³⁶ or APEX2,³⁷ data reductions, SAINTPLUS, version 6.63,³⁸ absorption correction, SADABS,³⁹ structural solutions, SHELXS-97,⁴⁰ structural refinement, SHELXL-97,⁴¹ graphics and publication materials, Mercury, version 2.3.⁴²

Synthesis of [(IMes)Fe(CO)(NO)₂]. 1,3-Bis(2,4,6-trimethylphenyl)imidazolium chloride (0.17 g, 0.50 mmol) and Na^oBu (0.048 g, 0.50 mmol) were combined and dissolved in THF under

N₂. The resulting solution was stirred for 30 min and then added by cannula under a positive pressure of N₂ at ambient temperature to a freshly prepared THF solution of Fe(CO)₂(NO)₂ (0.50 mmol).³⁵ The mixture was stirred for an additional 1 h and monitored by IR spectroscopy to confirm completion of the reaction. The solution was filtered through Celite to remove precipitated NaCl and dried under vacuum to yield spectroscopically pure product **2** (yield: 0.21 g, 92%). Dark-brown crystals suitable for X-ray analysis were grown by slow evaporation of a diethyl ether solution of complex **2** at –35 °C. IR (THF, cm⁻¹): ν(CO) 1986 (s); ν(NO) 1744 (s), 1702 (vs). ¹H NMR (CD₃CN): δ 7.41 (s, NCH), 7.06 (s, *m*-CH₃ of Mes), 2.32 (s, *p*-CH₃), 2.04 (s, *o*-CH₃). Anal. Found (Calcd for C₂₂H₂₄FeN₄O₃): C, 58.74 (59.09); H, 5.72 (5.77); N, 13.15 (13.32).

Synthesis of [(IMes)Fe(NO)₃][BF₄]. (1). A diethyl ether solution of complex **2** (0.23 g, 0.50 mmol), freshly prepared as described above, was transferred by cannula to a 50 mL Schlenk flask loaded with [NO]BF₄ (0.058 g, 0.50 mmol) at ambient temperature. The heterogeneous mixture was stirred overnight at RT and filtered to remove the solution from the precipitate. The green solid thus obtained was dissolved in THF; its IR spectrum indicated the formation of complex **1**. The green solid was washed successively with pentane (3 × 10 mL) to further remove impurities (yield: 0.19 g, 72%). Recrystallization in THF/pentane at –35 °C afforded crystals of complex **1** suitable for X-ray crystallographic study. IR (THF, cm⁻¹): ν(NO) 1932 (s), 1831 (s), 1804 (vs). ATR-IR (solid, cm⁻¹): ν(NO) 1916 (s), 1823 (vs), 1799 (vs). ¹H NMR (CD₃CN): δ 7.42 (s, NCH), 7.20 (s, *m*-CH₃ of Mes), 2.39 (s, *p*-CH₃), 2.11 (s, *o*-CH₃). Anal. Found (Calcd for C₂₁H₂₄BF₄FeN₅O₃): C, 47.37 (47.31); H, 5.08 (4.87); N, 12.53 (12.20).

Synthesis of [(IMes)Fe(SPh)(NO)₂]. (3). Complex **1** (0.27 g, 0.50 mmol) was dissolved in 10 mL of THF, and the solution was cooled to 0 °C. To this solution was added via cannula a precooled solution of NaSPh (0.067 g, 0.50 mmol) in 10 mL of THF. The reaction mixture was stirred at 0 °C for 5 min, after which IR monitoring indicated that no starting material remained. The solution was filtered through Celite and dried under vacuum to yield spectroscopically pure product **3** (yield: 0.23 g, 85%). Deep-purple crystals suitable for X-ray analysis were grown by slow evaporation of a diethyl ether solution of complex **3** at –35 °C. IR (THF, cm⁻¹): ν(NO) 1763 (s), 1715 (vs). Anal. Found (Calcd for C₂₇H₂₉FeN₄O₂S): C, 61.87 (61.88); H, 5.21 (5.55); N, 11.40 (11.08).

NO Capture by the NO Trapping Agent upon Reaction of Complex 1 and NaSPh. Inside the glovebox, solid complex **1** (0.11 g, 0.20 mmol) and NaSPh (0.027 g, 0.20 mmol) were put in a vial, which was then placed in a larger tube containing a MeOH solution (8 mL) of [(bme-dach)Fe]₂ (0.055 g, 0.10 mmol). The tube was capped with a well-sealed septum and cooled to 0 °C. THF solvent was then added to the inner vial of the reaction mixture by syringe. The reaction system was slowly warmed to room temperature and stirred for 8 h. The outer MeOH solution was collected and the solvent removed under vacuum. The residue was redissolved in 15 mL of CH₂Cl₂ and filtered through Celite. A band at 1647 (s) cm⁻¹ indicated the formation of the complex (bme-dach)Fe(NO).²⁶ The green filtrate was concentrated to 5 mL under vacuum, and addition of 30 mL of pentane resulted in the precipitation of the green solid (bme-dach)Fe(NO) (yield: 0.05 g, 82%). The IR spectrum of the contents of the inner vial showed ν(NO) bands at 1763 and 1715 cm⁻¹, indicating the presence of complex **3**.

Direct Mixing of Complex 1 and the NO Trapping Agent without NaSPh. Complex **1** (0.11 g, 0.20 mmol) and [(bme-dach)Fe]₂ (0.055 g, 0.10 mmol) were loaded into a septum-sealed 50 mL Schlenk flask, and 10 mL THF solvent was added by syringe. The reaction mixture was stirred for 10 min; its IR spectrum (THF solution) contained ν(NO) bands at 1795 (s), 1763 (s), and 1740 (vs) cm⁻¹ (Figure S9 in the Supporting Information). Addition of diethyl ether to the THF solution yielded a dark-brown precipitate, which was washed successively with diethyl ether (3 × 20 mL) to further remove impurities (yield: 0.09 g, 87%). Recrystallization in THF/pentane/diethyl ether at –35 °C afforded crystals of

- (35) McBride, D. W.; Stafford, S. L.; Stone, F. G. A. *Inorg. Chem.* **1962**, *1*, 386–388.
 (36) SMART: Program for Data Collection on Area Detectors, version 5.632; Bruker AXS Inc.: Madison, WI, 2005.
 (37) APEX2, version 2009.7.0; Bruker AXS Inc.: Madison, WI, 2007.
 (38) SAINTPLUS: Program for Reduction of Area Detector Data, version 6.63; Bruker AXS Inc.: Madison, WI, 2007.
 (39) Sheldrick, G. M. SADABS: Program for Absorption Correction of Area Detector Frames; Bruker AXS Inc.: Madison, WI, 2001.
 (40) Sheldrick, G. M. SHELXS-97: Program for Crystal Structure Solution; Universität Göttingen: Göttingen, Germany, 1997.
 (41) Sheldrick, G. M. SHELXL-97: Program for Crystal Structure Refinement; Universität Göttingen: Göttingen, Germany, 1997.
 (42) Mercury; Macrae, C. F.; Edgington, P. R.; McCabe, P.; Pidcock, E.; Shields, G. P.; Taylor, R.; Towler, M.; van de Streek, J. *J. Appl. Crystallogr.* **2006**, *39*, 453–457.

complex **4** suitable for X-ray crystallographic study. IR (THF (CH_2Cl_2), cm^{-1}): $\nu(\text{NO})$ 1795 (1806) (s), 1763 (1771) (s), 1740 (1746) (vs). ESI-MS+ (CH_2Cl_2): m/z 419.9 $[(\text{NO})\text{Fe}(\text{bme-dach})\text{Fe}(\text{NO})_2]^+$.

Reaction of Complex 3 and $[\text{NO}]\text{BF}_4$. Complex **3** (0.11 g, 0.20 mmol) and $[\text{NO}]\text{BF}_4$ (0.024 g, 0.20 mmol) were loaded into a 50 mL Schlenk flask, and the solids were dissolved in THF under a N_2 atmosphere. The color of the solution mixture immediately changed from purple to green. A THF-solution IR spectrum displaying bands at 1932 (s), 1831 (s), and 1804 (vs) cm^{-1} indicated the formation of complex **1**. As a byproduct, diphenyl disulfide was isolated (short column chromatography; silica gel and diethyl ether as eluent) and characterized by ^1H NMR spectroscopy and electron impact mass spectrometry (EI-MS).

Reaction of Complex 3 and CO(g). Carbon monoxide was bubbled into a 20 mL THF solution of complex **3** (0.053 g, 0.10 mmol) in a 100 mL Schlenk flask for 10 min. The flask was sealed under a 1 atm CO atmosphere and stirred overnight at room temperature. The reaction was monitored by IR spectroscopy. The IR spectrum in THF [$\nu(\text{CO})$ 1986 (s); $\nu(\text{NO})$ 1744 (s), 1702 (vs) cm^{-1}] matched that of complex **2**. Diphenyl disulfide was isolated as above and characterized by ^1H NMR spectroscopy and EI-MS.

Synthesis of $[(p\text{-Tolyl})_3\text{P}]\text{Fe}(\text{NO})_3[\text{BF}_4]$. In the same manner as described for **1**, the complex $[(p\text{-tolyl})_3\text{P}]\text{Fe}(\text{NO})_3[\text{BF}_4]$ was prepared by reaction of $(p\text{-tolyl})_3\text{P}]\text{Fe}(\text{CO})(\text{NO})_2$ [freshly prepared by reaction of $\text{Fe}(\text{CO})_2(\text{NO})_2$ (0.50 mmol)³⁵ and $(p\text{-tolyl})_3\text{P}$] with NOBF_4 (0.058, 0.50 mmol) in diethyl ether solution, which resulted in rapid precipitation of a dark-green solid. The dark-green solid was washed successively with pentane (3×10 mL) to further remove impurities (yield: 0.17 g, 62%). ATR-IR (solid, cm^{-1}): $\nu(\text{NO})$ 1917 (s), 1838 (vs), 1813 (vs). Anal. Found (Calcd for $\text{C}_{21}\text{H}_{21}\text{BF}_4\text{FeN}_3\text{O}_3\text{P}$): C, 45.61 (45.30); H, 3.83 (3.77); N, 7.60 (7.32).

Reaction of $[(p\text{-Tolyl})_3\text{P}]\text{Fe}(\text{NO})_3[\text{BF}_4]$ with NaSPh. The $[(p\text{-tolyl})_3\text{P}]\text{Fe}(\text{NO})_3[\text{BF}_4]$ salt (0.11 g, 0.20 mmol) and NaSPh (0.027

g, 0.20 mmol) were combined and dissolved in THF under N_2 at 0 °C. The reaction mixture was stirred for 15 min, after which IR monitoring indicated that no starting material remained. The resulting products were assigned by IR spectroscopy as a mixture of Roussin's red ester $(\mu\text{-SPh})_2[\text{Fe}(\text{NO})_2]_2$ [$\nu(\text{NO})$ 1783 (vs), 1756 (vs) cm^{-1} in THF] and $(p\text{-tolyl})_3\text{P}]\text{Fe}(\text{NO})_2$ [$\nu(\text{NO})$ 1716 (s), 1672 (vs) cm^{-1} in THF].

Direct Mixing of $[(p\text{-Tolyl})_3\text{P}]\text{Fe}(\text{NO})_3[\text{BF}_4]$ and the NO Trapping Agent. $[(p\text{-tolyl})_3\text{P}]\text{Fe}(\text{NO})_3[\text{BF}_4]$ (0.11 g, 0.20 mmol) and $[(\text{bme-dach})\text{Fe}]_2$ (0.055 g, 0.10 mmol) were loaded in a septum-sealed 50 mL Schlenk flask, and 10 mL of THF solvent was added by syringe. The reaction mixture was stirred for 10 min; its IR spectrum in THF contained $\nu(\text{NO})$ bands at 1795 (s), 1763 (s), and 1740 (vs) cm^{-1} , indicating the formation of complex **4**. The THF solution was filtered through Celite to remove the insoluble solid. Addition of diethyl ether to the THF solution yielded a dark-brown precipitate, which was washed successively with diethyl ether (3×20 mL) to further remove impurities (yield: 0.06 g, 54%).

Acknowledgment. We appreciate financial support from the National Science Foundation (CHE-0910679 to M.Y.D.) and the R. A. Welch Foundation (A-0924). We especially thank Dr. Joseph H. Reibenspies (TAMU) for his help with X-ray studies. We also thank the Laboratory for Biological Mass Spectrometry (TAMU) for the EI- and ESI-MS.

Supporting Information Available: X-ray crystallographic data (CIF) from the structure determinations, ORTEPs and full lists of metric parameters for complexes **1–4**, and the IR spectrum of complex **4**. This material is available free of charge via the Internet at <http://pubs.acs.org>.

JA104135X